Gust-detection from velocity azimuth display Doppler wind lidar profiling at the WiValdi research park.

Journal of Physics: Conference Series **2767** (2024) 092076 doi:10.1088/1742-6596/2767/9/092076

Gust-detection from velocity azimuth display Doppler wind lidar profiling at the WiValdi research park.

N Wildmann[1], J D Thayer[1], C Detring[2], E Päschke[2]

[1] Deutsches Zentrum für Luft- und Raumfahrt e.V., Institut für Physik der Atmosphäre, Oberpfaffenhofen, Germany
[2] Deutscher Wetterdienst, Meteorological Observatory Lindenberg – Richard-Aßmann-Observatory, Lindenberg, Germany

E-mail: norman.wildmann@dlr.de

Abstract. This study presents a new retrieval for gusts from Doppler wind lidar (DWL) velocity azimuth display (VAD) scans. The scanning mode which is presented allows for retrieval of mean wind speed, vertical wind speed, turbulence kinetic energy and peak gust speed with a single strategy. It is validated against sonic anemometer measurements at 90 m above ground and a reference DWL gust mode with faster scanning speed at the boundary-layer field site Falkenberg of the DWD. The new algorithm is then run on a multi-year dataset to obtain statistics of gusts at the WiValdi research park. It enables analyses not only at hub height, but also up to 500 m aloft with a reasonable availability above 60%. A case study of a convective cold pool shows the potential of the method to detect and analyze the vertical and horizontal structure of gusts with the proposed method. It highlights the importance of measurements throughout the boundary layer to understand the related physical processes to wind ramps and gusts.

1. Introduction

Turbulent flow in the atmospheric boundary layer (ABL) defines the loads on wind turbines, but measuring all of its components on the wide range of scales remains a challenge. For blade loads, transient winds and ramps, their intensity and spatial extent are of particular interest [1, 2]. If gusts can be detected and their propagation predicted, control strategies can be developed to minimize loads [3, 4, 5]. The types of gusts are divided into continuous gusts, which are described by statistical turbulence models such as the von Kárman model or the Dryden model, and discrete gusts, such as the extreme coherent gusts described in the IEC 61400-1 [6]. Beyond the extreme coherent gust, a variety of other types of coherent gusts occur that do not necessarily fall under either of the standardized definitions but cause specific loads and control challenges [7]. In operational meteorology, the World Meteorological Organization (WMO) defines gusts as the 'maximum value, over the observing cycle, of the 3-second running average wind speed'. With in situ instrumentation such as cup or sonic anemometers, the running average can be calculated from the time series. This is typically done at 10 m above ground with automatic weather stations. To get in situ observations at hub height of wind turbines, masts are required. Recent studies show that Doppler wind lidars (DWL), which

are becoming increasingly popular in wind energy applications, can be used for gust detection [8, 9]. The ease of deployment of DWL is a big advantage over mast installations and DWL can additionally provide measurements at higher altitudes and throughout the ABL. It is thus of great interest to obtain variables from DWL which are comparable to the well-established in situ instruments. A fast, continuous scanning mode (from here on 'fast gust', FG mode) can be used for DWL gust measurements equivalent to the WMO definition [9]. In this study, we want to show a gust retrieval from a slow continuous velocity-azimuth display (VAD) scan (from here on 'slow gust', SG mode). Latter has already been shown to be particularly useful for the retrieval of turbulence variables such as turbulence kinetic energy (TKE), its dissipation rate and integral length scale [10, 11]. Expanding the list of variables to include a gust value makes it possible to provide an additional component for describing turbulent flows using the SG mode. Calculating all variables from the same scanning configuration without changing modes reduces the complexity of the experimental setup and increases the continuity and availability of each variable. For the validation of the SG mode retrieval, data from the boundary-layer field site Falkenberg of the German Meteorological Service (DWD) are used. At the site, a 99-m mast and three DWLs were run in parallel to compare different scanning strategies and lidar systems from different manufacturers. For site assessment of an actual wind energy site, data from a DWL at a the research wind park WiValdi is used. Here as well, sonic anemometer data at hub height is available from a mast for comparison. Section 2 describes the gust retrievals and the experimental sites. In Sect. 3 the validation of the retrieval and a case study of a convective cold pool gust are presented.

2. Methods

2.1. Experiment description

2.1.1. Falkenberg At the boundary layer field site (in German: Grenzschichtmessfeld, GM) Falkenberg operated by the Meteorological Observatory Lindenberg - Richard Aßmann Observatory (MOL-RAO) of the German Meteorological Service (Deutscher Wetterdienst, DWD), micrometeorological measurements are performed. GM Falkenberg is located 5 km south of the Lindenberg observatory site, which is approximately 65 km southeast of Berlin. The field site is situated in flat terrain and mainly surrounded by agricultural land. For this study, data from the 99-m high meteorological tower equipped with sonic anemometers at 50.3 m and 90.3 m is used. These ultrasonic anemometers are manufactured by Metek (factory version USA-1) and resolve the wind vector with a high temporal resolution of 20 Hz. In addition, two Doppler lidar systems of type StreamLine from the manufacturer HALO Photonics (nowadays HALO Photonics by Lumibird) are operated in close proximity to the mast ($< 100\ m$) and run in FG and SG mode, respectively.

2.1.2. WiValdi At the research park wind energy WiValdi at Krummendeich in Northern Germany (`https://forschungspark-windenergie.de/`), a Leosphere (nowadays Vaisala) Windcube 200S has been measuring vertical profiles of wind since November 2020 [12]. Only recently in 2023, meteorological masts and two 4.2 MW Enercon E115 EP3-E4 wind turbines were installed. Data from 2021-2023 is used for statistics. The DWL was placed at a site approximately 1 km east of the reference mast that measures the inflow of the research park.

2.2. FG mode

One possible approach that enables directly the derivation of wind gusts from individual DWL scans requires a very fast scan with $t_s = 3.4$ s per round (hereafter referred as FG mode) to capture those very short-lived phenomena satisfying the WMO gust definition. The practical implementation of such a fast scan requires low pulse averaging (N = 3000) and implies a relatively high azimuthal resolution ($\Delta\theta \approx 33°$) [9]. The elevation angle of 62° was chosen in

analogy to the work of [8]. Figure 1a shows a sketch of the FG mode. Prior to the wind gust retrieval, filtering of the raw data is needed to remove erroneous radial velocity measurements to improve the accuracy of the final wind products [13]. For each scan circle, consisting of 10-11 independent radial velocity measurements, the wind speed is calculated using the sine wave fitting method. With one scan lasting 3.4 s, the number of independent radial velocity measurements used for the retrieval effectively mimics a 0.25 s sampling rate, similar to the recommendation of the WMO for an analog anemometer [14]. From the retrieved wind speeds of all single scans, the maximum within a 10-minute interval can be determined.

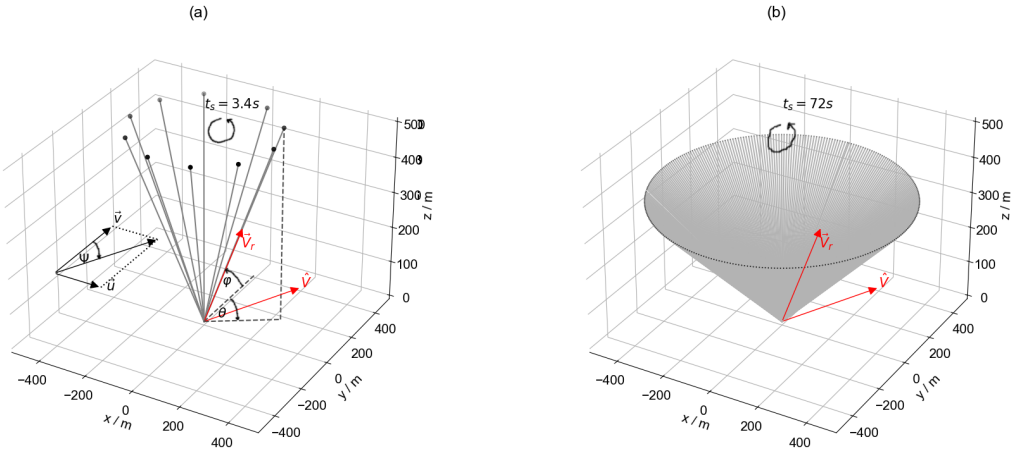

Figure 1. Sketch of the two lidar scanning modes FG (a) and SG (b). In (a) the wind vector u and v as well as the elevation φ and azimuth angle θ are visualized along with the radial velocity V_r and the projected velocity $\hat{V}$ in red.

2.3. SG mode

To retrieve accurate wind speeds, TKE and momentum fluxes, Smalikho and Banakh (2017) [10] developed and in further studies Wildmann et al. (2020) [11] used methods featuring a slow VAD scan at the mathematically optimal elevation angle $\sigma = 35.3°$. A high angular resolution is required to determine the azimuthal structure function, which is used to estimate dissipation rate and correct for volume averaging effects of the DWL. At GM Falkenberg, an azimuthal resolution $\Delta\theta = 1°$ ($\Delta t = 200$ ms accumulation time at $5°/s$) and at WiValdi a resolution of $\Delta\theta = 2°$ ($\Delta t = 400$ ms accumulation time at $5°/s$) was run. This high angular resolution leads to a long time period ($t_s = 72$ s) for a full 360° scan, hence why we call the method SG mode. Figure 1b shows a sketch of the setup.

VAD retrievals are based on the geometric projection of the wind vector onto the line-of-sight (LOS) of the laser beam and thus the radial velocity $V_r = \mathbf{S} \cdot \mathbf{V}$ [15], where $\mathbf{S} = \{\cos\varphi\cos\theta, \cos\varphi\sin\theta, \sin\varphi\}$ and $\mathbf{V} = \{u, v, w\}$. Retrieving gusts from the SG mode can be done by the use of individually-projected LOS velocities. This is in contrast to methods such as the FG mode that first calculate the wind vector for a full revolution. If the wind direction Ψ is known, and vertical wind w is assumed to be small, the VAD equation can be simplified and solved for the absolute wind speed

$$\hat{V} = V_r \cos\varphi^{-1} \cos(\Psi - \theta)^{-1} \tag{1}$$

Figure 2a shows the typical sine shape of measured radial velocities. It is evident that a few radial velocities deviate significantly from the mean cosine fit at the respective azimuth angle θ. In order to match the WMO definition of gusts, the lidar scan is averaged with a running average filter of $\Delta t \approx 3$ s. For WiValdi, a filter of 2.8 s is used, which equals seven LOS measurements. For GM Falkenberg, 15 LOS values are used. From the averaged projected velocities $\hat{V}$, the maximum $\hat{V}_{\max}$ within a 10-minute time window is determined. Large uncertainties in the geometrical projection can occur at angles $\Delta\theta_c = |\Psi - \theta|$ close to 90°, which is why an angular range of ±45° around the singularity is excluded from the analysis (grey areas in Fig.2a). This means that single, small events can potentially be missed in the blind phases of the scans.

In the analyses, it needs to be considered that the DWLs only have a limited detector

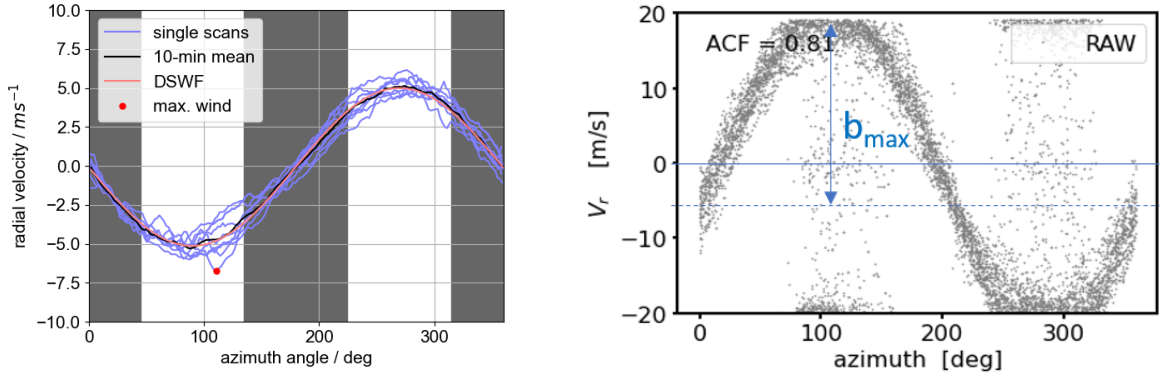

Figure 2. a) VAD radial velocities from single scans (purple), 10-minute average (black) and the corresponding direct sine-wave fit (DSWF, orange). The grey shaded areas are the angles that are excluded from the analysis. The red dot shows the detected maximum wind speed b) VAD of observed Doppler velocities (V_r) for a 30-minute measurement interval where the true amplitude of the sine-wave cannot be captured due to range aliasing effects.

bandwidth, which determines the maximum radial velocities that can be measured. For the Halo Streamline lidars it is $V_{\mathrm{r,max}} = \pm 19$ m/s; for the Leosphere Windcube 200S it is $V_{\mathrm{r,max}} = \pm 30$ m/s. Hence, fitting VAD data from the SG mode ($\varphi = 35.3°$) to a general sine equation with b denoting the amplitude, the maximum horizontal wind speed can be derived as $V_{\mathrm{hor,max}} = b_{max}/\cos\varphi$, i.e. 23 m s^{-1} and 37 m s^{-1} for the two types of DWL respectively. Note, here it has been assumed that $w = 0$, which implies $b_{max} = V_{\mathrm{r,max}}$ with b_{max} denoting the maximum resolvable amplitude due to the limitations of the receiver bandwidth. The SG mode is in disadvantage to the FG mode in that respect, because the higher elevation angle ($\varphi = 62°$) in FG mode allows higher maximum horizontal wind speeds (40 m s^{-1} for Halo Streamline). Figure 2b shows the VAD of a Halo Streamline in SG mode at its operational limits. Note that here the shift of the sine along the V_r axis indicates vertical wind speeds $w \neq 0$ yielding $b_{max} > V_{\mathrm{r,max}}$, which would shift the limit for $V_{\mathrm{hor,max}}$ towards somewhat higher values.
At Falkenberg, the SG mode is run continuously with a DWL. At the WiValdi site, the SG mode alternates in 30-minute periods with a VAD scan with the same configuration, but at an elevation angle of 75° to observe higher profiles and higher maximum wind speeds.

3. Results

3.1. Validation of DWL gust retrievals

3.1.1. Comparison with sonic anemometers In order to evaluate the applicability of the lidar gust retrievals, the most straightforward way is to compare the retrieved mean and peak wind

speeds in 10-minute intervals to the long-term established measurements at the 99-m mast at GM Falkenberg. We use a 3-month period from 20 January through 20 April 2022 and calculate a linear regression between sonic and FG mode, as well as sonic and SG mode. After filtering wind direction angles in which the sonic anemometer is subject to shadowing effects and DWL data filtering according to [13], a high correlation of $R \geq 0.96$ is achieved for both mean and peak velocity (see Fig. 4). Using the SG retrieval for gust measurements at the WiValdi site reveals similarly good results ($R > 0.97$, not shown).
We investigate the sensitivity of the SG method to the cutoff angle for the geometric projection, see Fig. 3. It shows that the root-mean-square deviation (RMSD) decreases and the correlation

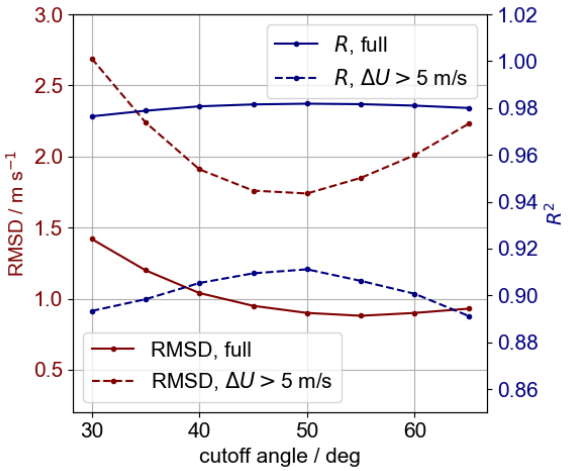

Figure 3. RMSD (red) and correlation coefficient R (blue) in dependency of the cutoff angle for geometrical LOS reconstruction. The solid curves show the values for the full dataset and the dashed curves only for the subset with gust amplitudes $\Delta U > 5$ m s^{-1}.

coefficient R increases up to 50° for the full dataset and the subset with gust amplitudes $\Delta U > 5$ m s^{-1}. That indicates that error propagation through the geometric projection yields large errors for azimuth angles deviating far from the wind direction, but also shows that most gusts are big enough to be well captured even when large angle ranges are disregarded. The error does increase again for higher angles $\Delta\theta_c$. This can be explained by the bandwidth-limitations at high wind speeds as explained in Sect. 2.3 but partially also because small, short-lived gusts may be missed. We chose $\Delta\theta_c = 45°$ as the smallest cutoff angle for which the RMSD falls below 1 m s^{-1}. Figure 5 shows a direct comparison of FG mode and SG mode at 90 m. A good comparison between the two modes can be confirmed at such low altitudes. The differences in the scattering between the mean wind plots and the max gust speed plots illustrate, however, the higher uncertainty of both modes in wind gust determination than for the mean wind estimate.

3.1.2. Intercomparison of lidar gust measurements above 90 m Since the VAD cone covers a much larger area at greater heights, it is important to look at the comparison also aloft. While the FG mode has a radius of the scan circle of only 132 m at 250 m height, the SG mode has 357 m at the same height. For the FG mode, it can be considered more important to have the small radius because an average over the cone is done to obtain a single wind profile. Figure 6 shows the regression at 250 m with no significant reduction in agreement between the two modes in comparison to the results shown for 90 m (Fig. 5). It is noticeable, however, that for higher

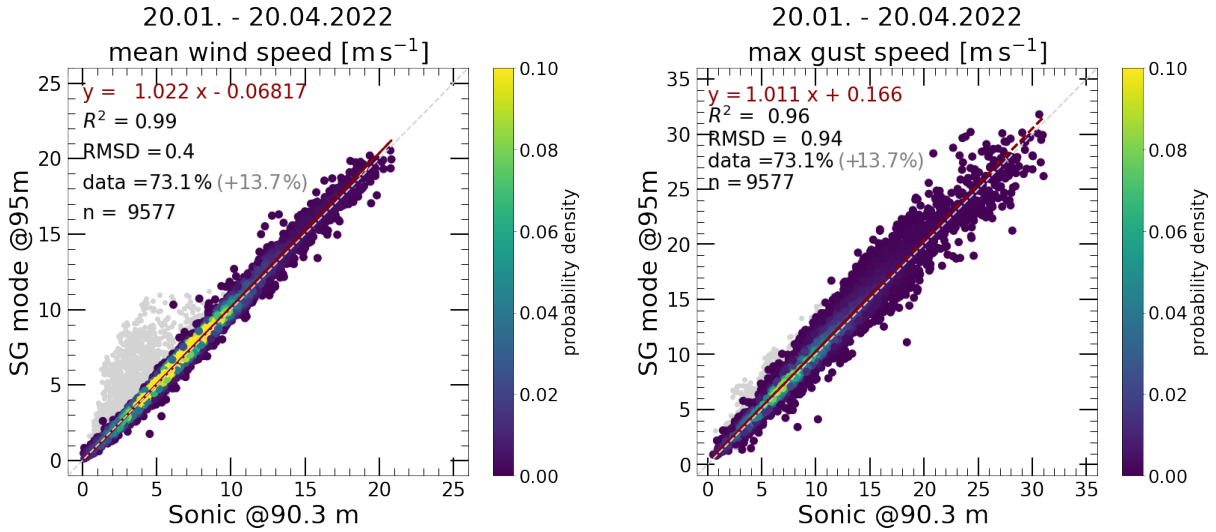

Figure 4. a) Scatter plot of mean wind speed in 10-minute intervals of the sonic at 90 m compared to the SG mode for the time period 20 January to 20 April 2022. b) The same comparison, but with maximum (gust) wind speed. Grey dots: without quality flag; colored: with quality flag.

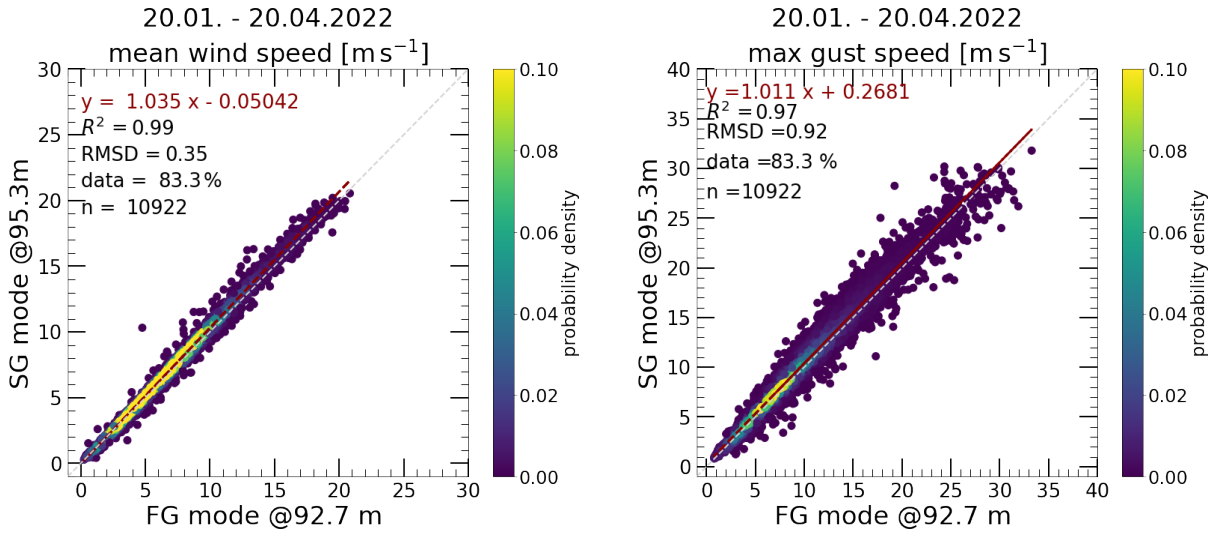

Figure 5. a) Scatter plot of mean wind speed in 10-minute intervals of the FG mode compared to the SG mode for the time period 20 January to 20 April 2022. b) The same comparison, but with maximum (gust) wind speed.

wind speeds (> 20 - 22 m/s) there is a tendency of saturation in the measured mean wind and gust speeds from the SG mode. This can be explained by the DWL bandwidth limitations as discussed in Sec. 2.3.

3.2. Gusts at the WiValdi wind site

3.2.1. Long-term statistics The WiValdi site at Krummendeich is just like the GM Falkenberg: a site in flat terrain with heterogeneous land cover in the environment. In contrast to Falkenberg,

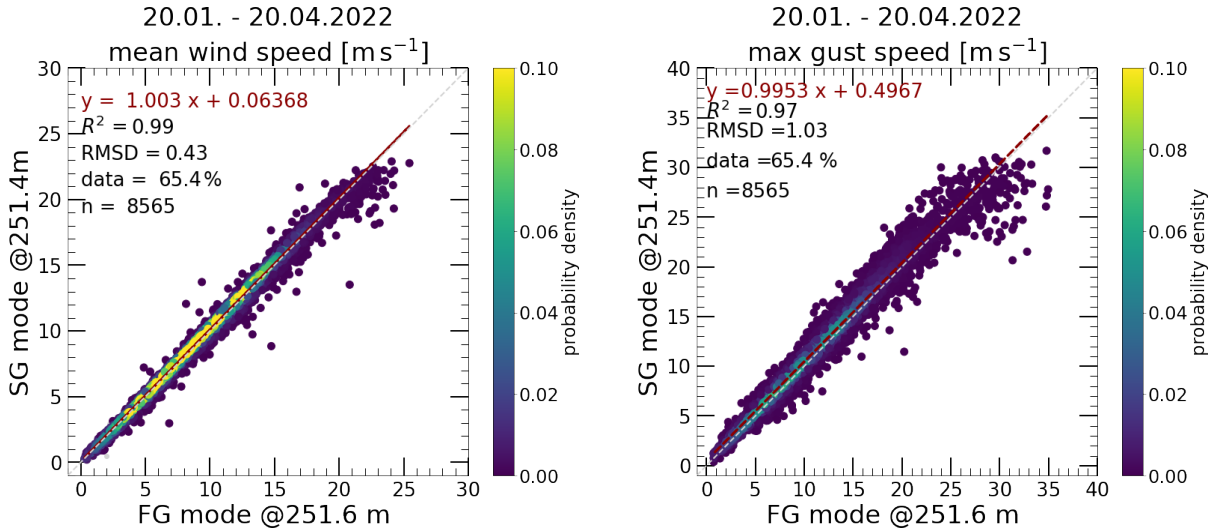

Figure 6. a) Scatter plot of mean wind speed in 10-minute intervals of the FG mode compared to the SG mode for the time period 20 January to 20 April 2022 in / 250 m height. b) The same comparison, but with maximum (gust) wind speed.

Krummendeich is closer to the coast of the North Sea (approx. 40 km) and exhibits much larger wind speeds at lower altitudes. In Wildmann et al. (2022) [12], statistics of wind speed, stability and low level jet (LLJ) occurrence was presented. With the new gust retrieval, we can now also present gust peak velocity and gust amplitude in dependence of wind direction for an even longer time period. The wind roses in Fig. 7 only show gust peak velocity and amplitude above 5 m s^{-1}. It is obvious that strong winds and high gust amplitudes are mostly observed from the West.

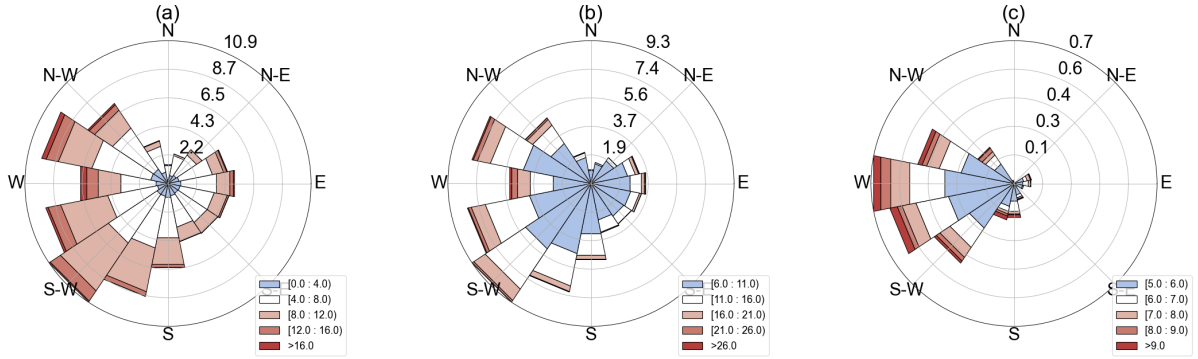

Figure 7. Wind rose of the mean wind speed (a) gust peak wind speed (b) and the gust amplitude (c) for the time period January 2021 through December 2023 at 100 m height.

3.2.2. Dependency on height To evaluate the dependency of gust statistics on height, we show probability density functions at 60 m, 100 m, 200 m and 500 m (see Fig. 8). The gust peak distributions are fitted to a lognormal distribution and the gust amplitude to a Weibull distribution as in Hu et al. (2018) [1]. The curves that Hu et al. determined for a site in moderately complex terrain in the state of New York in the USA are also shown for comparison (dashed lines). It shows that the gust peak velocities increase with height as expected while

the gust amplitudes slightly decrease. In comparison to Hu et al. (2018), the site in Northern Germany is less gusty, with a lower probability of high amplitude gusts even at 100 m above ground.

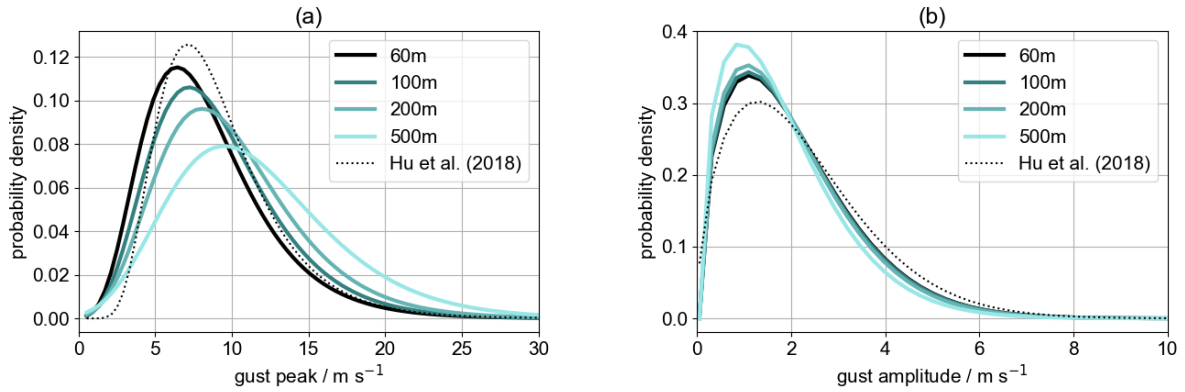

Figure 8. Histogram of the gust peak wind speed (a) and the gust amplitude (b) for the time period 24 March to 23 May 2023 and heights between 60 m and 500 m. As a reference, the PDF as reported by Hu et al. (2018, dashed line) is shown.

3.2.3. Case study, 03 July 2023 From the statistics of gust measurements, we learn about site-specific characteristics. We saw that strong gusts do appear at the site with highest probability in conditions with south-westerly winds. One common mechanism for gusts is that stronger winds aloft are mixed down to the ground by convection. Such events can cause significant wind ramps, which are of high interest for loads on wind turbines. These discrete convective events cannot be predicted well by numerical models and measurements at a single height, such as with horizontal PPI lidar scans, can only show the gust as it reaches the lower levels. Therefore, the SG mode can potentially reveal more information about the development and structure of such gusts in three dimensions. To evaluate the possibilities, we look at a case study of measurements on 3 July 2023. On that day, strong upper-level west-southwesterly flow across northwest Germany drifted southeastward throughout the day with a frontal passage that was associated with a low-pressure system over Scandinavia. Shallow, cellular convection developed during the early daylight hours along this front as the boundary-layer instability gradually increased, allowing for the strong upper-level winds to mix downwards. Occasional convection and associated cold pools passed directly over the WiValdi wind park during this morning, observed through a succession of rapid increases in low-level wind speeds, rapid decreases in low-level temperature, and measurable rainfall. Figure 9a shows the time series of mean wind (solid) and peak gust velocity (dashed) at 100 m (red) for the DWL measurements and 85 m (black) for the sonic anemometer for comparison. It shows that at lower heights, the mean wind is mostly around 10 m s^{-1} between 04:00 UTC and 10:00 UTC, with a short increase to 13 m s^{-1} between 08:00 UTC and 10:00 UTC. A very evident peak is visible at 08:30 UTC in the gust velocity associated with a shower of rain shortly thereafter, which also corrupts vertical wind measurements. More than 20 m s^{-1} horizontal wind speed are measured by both the DWL and sonic, and at both heights. That denotes a gust amplitude of 8 m s^{-1}. The time-height plots of mean wind (b), vertical wind w (c) and gust amplitude (d) reveal the vertical structure of the atmosphere during this morning. In the early morning, a strong shear layer is present with high wind speeds above 500 m above ground. The PPI scan on the top right in Fig. 10a shows the situation at 06:58 UTC. The white contour lines indicate the height within the scan (100 m,

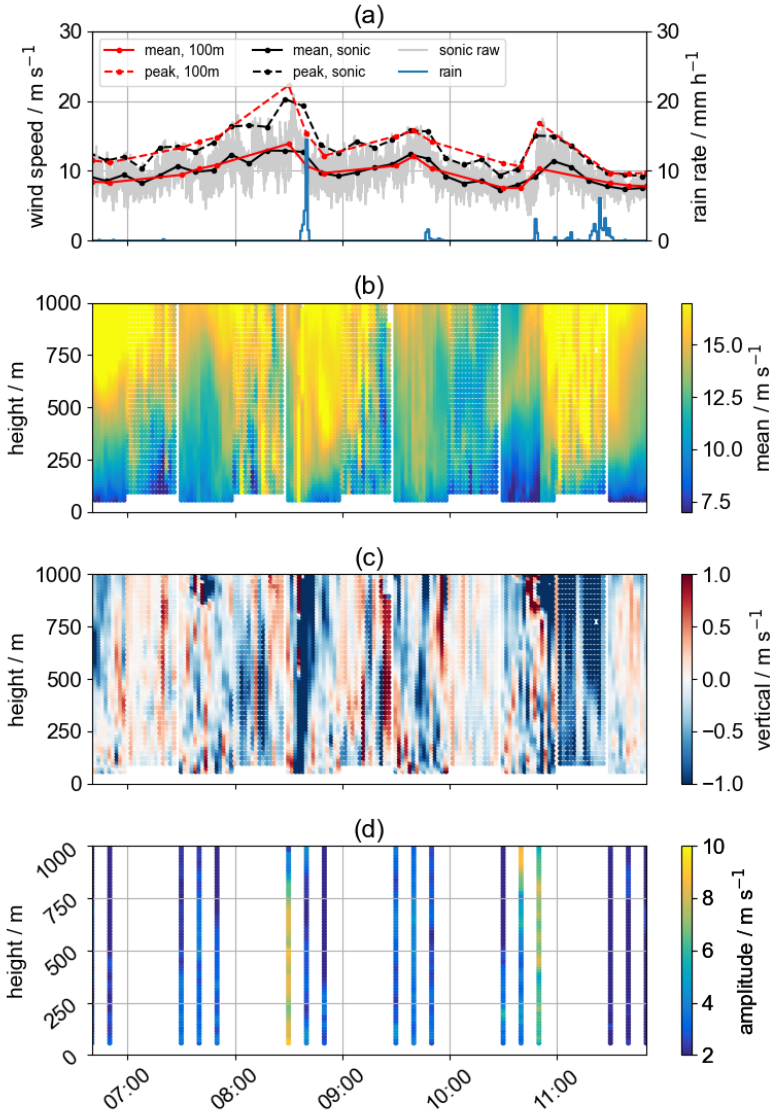

Figure 9. Time series of mean wind speed (solid) and gust peak velocity (dashed) for 03 July 2023, 06:45 UTC to 12:00 UTC (a) at 100 m (red) as well as sonic anemometer measurements at 85 m (black). The panels below show time-height plots of mean wind speed (b), vertical wind (c) and gust amplitude (d). Only data from VAD scans with 35° elevation are shown for the gust retrieval and 10-minute windows. Mean and vertical wind speed is shown with a 2-minute window and includes 75° elevation scans as well.

200 m, 500 m and 1000 m). Figures 10b and c show the situation during the gust event as it hits the lidar position from the South (08:37 UTC) and as it just passed over (08:39 UTC). The gust was accompanied by a cloud with a base height of 500 m, which limits the range of the lidar scan in those scans.

4. Conclusions

In this study, we introduced a new method to retrieve gusts from DWL measurements and use the data to gain more insight into discrete gust events, which are of particular interest for

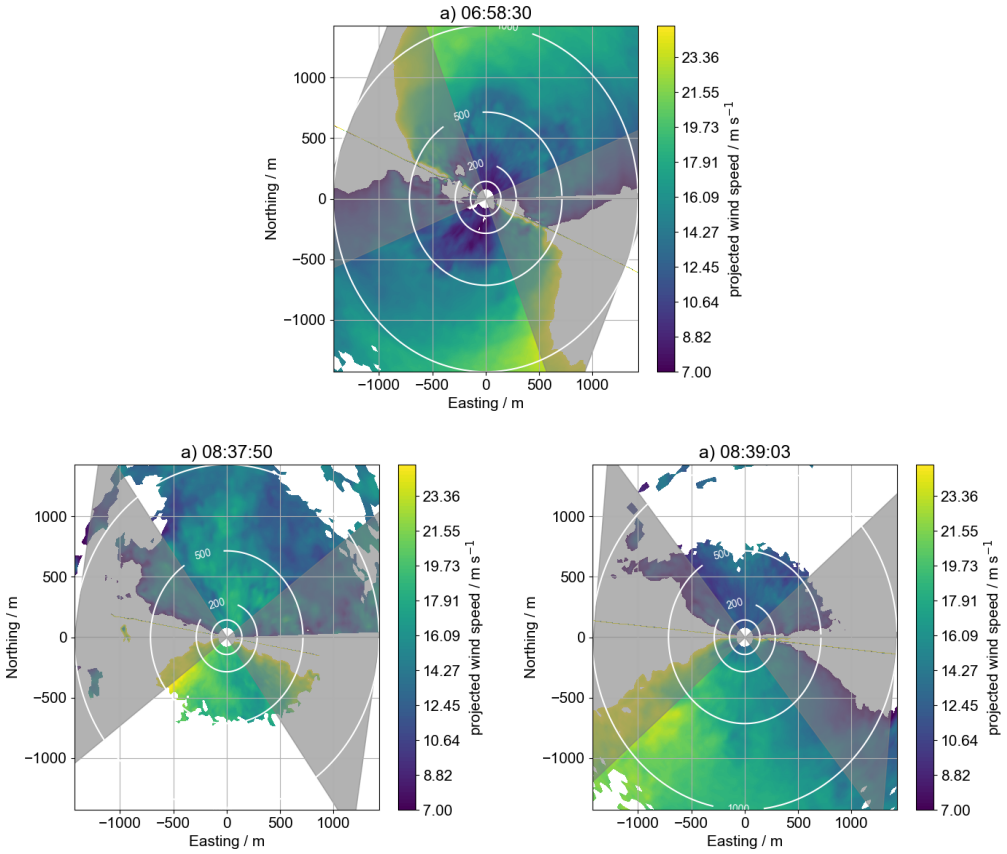

Figure 10. Three PPI scans of the VAD with 35° angle are shown: 06:58 UTC (a), 08:37 UTC (b) and 08:39 UTC (c). The white contour lines indicate the height of the data and the grey shaded areas are those areas which are excluded from the LOS analysis due to constraints in the geometric projection.

load characterization of wind turbines and ramps in the energy production of wind parks. We showed that with the SG mode, which was originally designed to retrieve mean wind speed and TKE, it is also possible to observe a gust variable with good accuracy (RMSD$\leq$ 1 m s^{-1}) and correlation ($R \geq 0.95$) in comparison to in situ observations according to the WMO definition. Additionally to the validation to a sonic anemometer, the method was also compared to the DWL FG mode which allows cross-validation at higher altitudes. No significant decline in accuracy was observed. Some findings are important to be considered if the method is applied:

- In contrast to the FG mode, the SG mode operates at a lower elevation angle. That means that the maximum wind speeds that can be detected due to instrument limitations are lower, but also depend on the detector bandwidth of the DWL type.
- A good filter method is even more crucial for the gust detection than for the mean wind speed or turbulence retrieval because single LOS radial velocities have a higher weight in gust estimation. We propose the filter using a correlation function of the smallest azimuthal increment as described in [13].
- The assumption of negligible vertical wind speed and constant wind direction within one VAD revolution can be violated in gusts and will thus feed into the uncertainty of the method.

- Lidar remote sensing is subject to availability issues, especially in foggy or cloudy conditions and in very clear air (no aerosol-backscatter). In our WiValdi dataset, availability at 100 m is just above 80 % (including downtime caused by technical issues) and decreases to just above 70% at 500 m during the day and 60% at night.

Given these boundary conditions and limitations, retrieving gusts from DWL opens a lot of opportunities for understanding loads and power fluctuations in wind parks, increasing the height range of observations and even allow to obtain spatial and temporal information about the gusts. More refinements can be implemented to the method in the future to retrieve parameters such as the gust length scale, shape, rise and lapse times, which were not shown in this study. Multiple studies have recently been carried out that assess the use of remote sensing for minute-scale power forecasting. Pichault et al. (2021) [16] made the case that a combination of remote sensing and machine learning can outperform persistence models. Valldecabres et al. (2020) [17] have used Doppler radar data in a similar approach. These approaches mainly focus on horizontally, forward-looking measurements at hub height. Lochmann et al. (2023) [18] investigated the applicability of vertically-profiling lidar measurements to improve short-term forecasts, but did not find significant improvements with standard profiling products of wind speed and wind direction, possibly because of too large a distance between the wind park and observations. It should be investigated in the future if our approach to detect gusts, turbulence and vertical wind can further improve short-term forecasting, especially for convectively-induced wind ramps. The statistical dataset we presented for the WiValdi site can be used for this purpose.
The case study of 3 July 2023 showed an interesting case of a convective cold pool developing in the lowest boundary-layer heights and causing a gust of 8 m s^{-1} amplitude. In the future, with operating wind turbines and sensors in all structural components of the turbines, the WiValdi infrastructure enables detailed analyses of the effects of a discrete gust on the loads and the control system.

Acknowledgements

This work was partly accomplished within the research project Deutsche Forschungsplattform für Windenergie (http://dfwind.de). We greatly acknowledge the financial support of the German Federal Ministry for Economic Affairs and Climate Action, through FKZ 0325936, that enabled this work.

References

[1] Hu W, Letson F, Barthelmie R J and Pryor S C 2018 *J. of Appl. Met. and Clim.* **57** 1459 – 1476
[2] Pichault M, Vincent C, Skidmore G and Monty J 2022 *J. of Wind Eng. and Ind. Aer.* **220** 104864 ISSN 0167-6105
[3] Schlipf D, Schlipf D J and Kühn M 2013 *Wind En.* **16** 1107–1129
[4] Zhou K, Cherukuru N, Sun X and Calhoun R 2018 *Remote Sensing* **10** ISSN 2072-4292
[5] Hannesdóttir A, Verelst D R and Urbán A M 2023 *Wind En. Sci.* **8** 231–245
[6] The International Electrotechnical Commission 2021 Tech. Rep. IEC 61400-15 IEC
[7] Hannesdóttir A and Kelly M 2019 *Wind En. Sci.* **4** 385–396
[8] Suomi I, Gryning S E, O'Connor E J and Vihma T 2017 *QJ of the Roy. Met. Soc.* **143** 2061–2072
[9] Steinheuer J, Detring C, Beyrich F, Löhnert U, Friederichs P and Fiedler S 2022 *Atm. Meas. Tech.* **15** 3243–3260
[10] Smalikho I N and Banakh V A 2017 *Atm. Meas. Tech.* **10** 4191–4208
[11] Wildmann N, Päschke E, Roiger A and Mallaun C 2020 *Atm. Meas. Tech.* **13** 4141–4158
[12] Wildmann N, Hagen M and Gerz T 2022 *J. Phys.: Conf. Ser.* **2265** 022029
[13] Päschke E and Detring C 2023 *Atm. Meas. Tech. Discussions* **2023** 1–53
[14] WMO 2021 (WMO) [last access: 16 March 2024] URL `https://library.wmo.int/idurl/4/68695`
[15] Smalikho I 2003 *Journal of Atmospheric and Oceanic Technology* **20** 276–291
[16] Pichault M, Vincent C, Skidmore G and Monty J 2021 *Energies* **14**
[17] Valldecabres L, von Bremen L and Kühn M 2020 *Wind En.* **23** 2202–2224
[18] Lochmann M, Kalesse-Los H, Schäfer M, Heinrich I and Leinweber R 2023 *Wind En.* **26** 573–588